Applied Physics B (2019) 125:211
https://doi.org/10.1007/s00340-019-7315-8

Applied Physics B
Lasers and Optics

A portable miniaturized laser heterodyne radiometer (mini-LHR) for remote measurements of column CH_4 and CO_2

E. L. Wilson[1] · A. J. DiGregorio[2] · G. Villanueva[3] · C. E. Grunberg[4] · Z. Souders[4] · K. M. Miletti[4] · A. Menendez[4] · M. H. Grunberg[4] · M. A. M. Floyd[5] · J. E. Bleacher[6] · E. S. Euskirchen[7] · C. Edgar[7] · B. J. Caldwell[8] · B. Shiro[9] · K. Binsted[10]

Received: 19 March 2019 / Accepted: 27 September 2019 / Published online: 21 October 2019

Abstract

We present the design of a portable version of our miniaturized laser heterodyne radiometer (mini-LHR) that simultaneously measures methane (CH_4) and carbon dioxide (CO_2) in the atmospheric column. The mini-LHR fits on a backpack frame, operates autonomously, and requires no infrastructure because it is powered by batteries charged by a folding 30 W solar panel. Similar to our earlier instruments, the mini-LHR is a passive laser heterodyne radiometer that operates by collecting sunlight that has undergone absorption by CH_4 and CO_2. Within the mini-LHR, sunlight is mixed with light from a distributive feedback (DFB) laser centered at approximately 1.64 μm where both gases have absorption features. The laser scans across these absorption features roughly every minute and the resulting beat signal is collected in the radio frequency (RF). Scans are averaged into half hour and hour data products and analyzed using the Planetary Spectrum Generator (PSG) retrieval to extract column mole fractions. Instrument performance is demonstrated through two deployments at significantly different sites in interior Alaska and Hawaii. The resolving power ($\lambda/\Delta\lambda$) is greater than 500,000 at 1.64 μm with precisions of better than 20 ppb and 1 ppm for CH_4 and CO_2, respectively. Because mini-LHR instruments are portable and can be co-located, they can be used to characterize bias between larger, stationary, column observing instruments. In addition, mini-LHRs can be deployed quickly to respond to transient events such as methane leaks or can be used for field studies targeting geographical regions.

✉ E. L. Wilson
Emily.L.Wilson@nasa.gov

[1] Atmospheric Chemistry and Dynamics Laboratory, NASA Goddard Space Flight Center, 8800 Greenbelt Road, Greenbelt, MD 20771, USA

[2] Science Systems and Applications, Inc., 10210 Greenbelt Rd, 20, Lanham, MD 20706, USA

[3] Planetary Systems Laboratory, NASA Goddard Space Flight Center, 8800 Greenbelt Road, Greenbelt, MD 20771, USA

[4] Center for Research and Exploration in Space Science and Technology (CRESST), University of Maryland, College Park, MD 20740, USA

[5] Planetary Environments Laboratory, NASA Goddard Space Flight Center, 8800 Greenbelt Road, Greenbelt, MD 20771, USA

[6] Planetary Geology, Geophysics, and Geochemistry Laboratory, NASA Goddard Space Flight Center, 8800 Greenbelt Road, Greenbelt, MD 20771, USA

[7] Institute of Arctic Biology, University of Alaska Fairbanks, 902 N. Koyukuk Dr, P.O. Box 757000, Fairbanks, AK 99775, USA

[8] Exploration Class Management, 414 Bayoo View Drive, El Lago, TX 73472, USA

[9] Department of Earth Sciences, University of Hawai'i at Mānoa, POST Building, Suite 701, 1680 East - West Road, Honolulu, HI 96822, USA

[10] Department of Information and Computer Sciences, University of Hawai'i at Mānoa, POST Building Suite 303D, 1680 East - West Road, Honolulu, HI 96822, USA

1 Introduction

We present a portable, miniaturized, laser heterodyne radiometer (mini-LHR) which is the latest iteration of an instrument that has been under development by our team since 2009 to monitor greenhouse gases (GHGs) in the atmospheric column [1–6]. The re-design of the mini-LHR into a portable unit was motivated by our first trip to the Bonanza Creek Research Forest near Fairbanks, AK where we were to make column measurements of CH_4 and CO_2 over thawing permafrost. During summer months, the various research sites are only accessible by trail and all equipment must be backpacked in. There is no electricity beyond what solar power can be packed in or brought in with a snow machine during winter months. After the first year at Bonanza creek, we put all of our resources into the backpack version of the mini-LHR with its own small solar power system.

Once we had developed the portable field unit, interesting opportunities arose including one that involved testing the new mini-LHR as part of the Hawai'i Space Exploration Analog and Simulation (Hi-SEAS) which is a long duration Mars analog simulation program operated by the University of Hawai'i at Mānoa. The site of the habitat is on the Mauna Loa side of the saddle area on the Big Island at ~ 8200 feet above sea level. Here, the crew of six uses the mini-LHR as a way to monitor atmospheric conditions like they would in a Mars deployment. Crew members live in a geodesic dome habitat and can only access the instrument during extravehicular activity (EVA) outings that require crewmembers to wear "space suits". Because these suits significantly limit manual dexterity, we added a touch screen interface that could be used with a stylus pen.

Fig. 1 Clockwise from bottom left: the mini-LHR and solar panel in its backpack harness, the trail to the black spruce and collapse scar bog permafrost sites at the Bonanza Creek Research Forest in interior Alaska, Hi-SEAS crewmembers pose with the mini-LHR on a pāhoehoe lava flow on Mauna Loa, and the mini-LHR collects CH_4 and CO_2 data at the fen permafrost site alongside a covariance flux tower at Bonanza Creek

Both Bonanza Creek and Hi-SEAS field sites (Fig. 1) are good test cases for the mini-LHR instrument because they differ in many respects including climate, altitude, the solar zenith angle, number of hours of sun per day, etc. They also provided different deployment obstacles. While both sites are important for column CO_2 and CH_4 monitoring, neither of these sites are good candidates for permanent structures—highlighting potential locations that the mini-LHR could supplement column measurements of networks like the total carbon column observing network (TCCON) which measures a wide range of atmospheric gases using Fourier Transform Spectrometers (FTS) at permanent installations [7].

While FTS instruments have been widely known as trace gas analyzers and have been commercially available since the 1960s, the same is not true for laser heterodyne radiometers which to date have not been commercialized. Laser heterodyne radiometry has been used to measure gases in the atmosphere since the early 1970s [8–14], but the lasers used in these ground-breaking instruments were large, expensive, complex systems that typically required high voltage–power supplies and pumped cooling systems. Another obstacle to commercialization was versatility. Because lasers emit light at a particular wavelength, a gas absorption feature must exist near the laser's output to be able to make the measurement. Typically, only a few atmospheric gases can be reached within the wavelength range of a single laser. While LHRs had superior spectral resolution and sensitivity to other instruments such as grating spectrometers or Fourier transform spectrometers, LHRs could measure as many gases in a single instrument.

In recent years, however, smaller, low-power, semiconductor lasers have become commercially available in infrared wavelengths that are able to reach more gas absorption features. These lasers are thermoelectrically cooled and are the size of a quarter. While it remains true that a single laser may only be able to measure a few gases, these lasers are cheap and small enough that multiple lasers can be used in a single instrument to expand the measurement capability as needed. Here, we detail our simple instrument design that measures CO_2 and CH_4 with a single laser at 1640 nm that can be expanded to measure other atmospheric gases.

We compare performance of two mini-LHR instruments at the Bonanza Creek and Hi-SEAS field sites and discuss how these instruments could be used to produce data products in hard to reach locations where long-term monitoring stations are impractical or too costly.

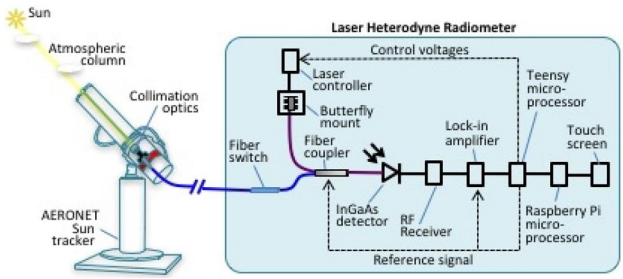

Fig. 2 Components of the mini-LHR. Mole fractions of CO_2 and CH_4 are found by measuring their absorption by sunlight in the infrared near 1.6 μm. Sunlight is collected with collimation optics that are connected to a sun tracker and modulated with a fiber switch. Sunlight is mixed with laser light to produce a beat signal that is detected and amplified with a RF receiver, and measured with a lock-in amplifier referenced to the modulation frequency. Absorption is measured by scanning the laser while monitoring the beat signal amplitude with the lock-in amplifier

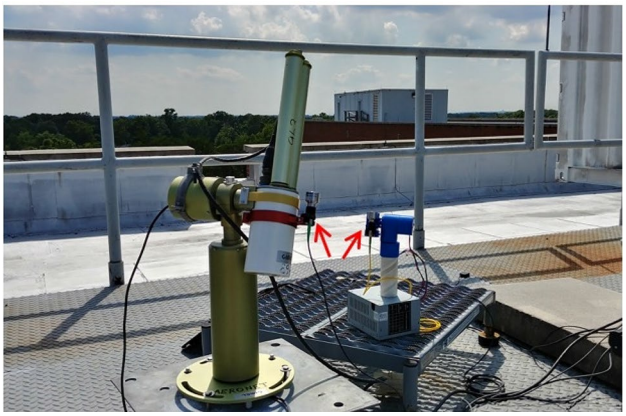

Fig. 3 Sunlight is collected with a fiber-coupled collimator connected to the sun tracker portion of an AERONET sun photometer (left). For field applications where an AERONET is not available, our smaller tracker (right) provides sun pointing. Collimators are indicated by red arrows

2 Instrument design

In our early designs, we packaged commercial components that were intended for benchtop use into waterproof cases and tested these in the field. While this approach was reasonable to validate that newly available distributive feedback (DFB) lasers could be used in laser heterodyne radiometers, it was not cost effective or particularly practical for future manufacturing. The design we present here has transitioned these commercial components to printed circuit boards that can be mass produced at a low cost to make mini-LHRs commercially viable as a field instrument.

A schematic of the mini-LHR is shown in Fig. 2. At the front end, sunlight that has undergone absorption by CO_2 and CH_4, is collected with a small fiber-coupled telescope (Thorlabs, F810APC-1550) with a focal length (*f*) of 7 mm and numerical aperture (NA) of 0.24 that mounts to the sun tracker portion of an AERONET sun photometer that has a pointing accuracy of 0.1° [15, 16]. For use with the mini-LHR, we use two AERONET tracking modes. For continuous tracking of the sun throughout the day, the AERONET sun tracker is operated in "BCLSUN" mode, which requires a user to start the tracker in the morning and turn the tracker off at night. This produces approximately 60 raw scans per hour in clear sky conditions that are averaged into either half hour or full hour data products. If a user is not available and the mini-LHR is operating autonomously for days or months, the AERONET sun tracker can be operated in "TURBO" mode and a raw scan is collected when the AERONET sun tracker points at the sun at 2 min intervals. This provides about 30 raw scans per hour that are averaged into 1 h data products.

Our preference is always to operate the mini-LHR in tandem with an AERONET instrument because this produces a satellite validation product of both aerosol optical depth (AOD) and column CH_4 and CO_2. However, in some situations, an AERONET sun tracker is not available at the site. For these situations, we use a custom in-house sun tracker that tracks continuously with a pointing accuracy of ~ 0.06° and can operate autonomously. Figure 3 shows an AERONET sun tracker (left) and our in-house tracker (right) with collimators indicated by red arrows.

Once collected with the collimator, incoming sunlight is modulated with a solid-state fiber optic switch at 400 Hz (Agiltron, CL 1 × 1) and then coupled with laser light in a single mode, wideband fiber optic coupler (Thorlabs, TW1650R5A1). Laser light is produced from a distributive feedback (DFB) laser (Eblana Photonics) that tunes between 1640.2 and 1640.5 nm to capture CO_2 and CH_4 absorption features. After coupling, laser light and sunlight are mixed in a > 15 GHz InGaAs detector (Electro-Optics Technology, ET-3500F). The resulting beat signal is detected in a custom RF receiver [2]. The RF receiver amplifies the RF signal, detects it with a square law detector, and then further amplifies it with a video amplifier. The output signal from the RF receiver is detected with a lock-in amplifier (Femto, LIA-MV-150) that is referenced to the 400 Hz modulation signal. Two low-cost microprocessors are used in this set-up: A Teensy 3.2 (pjrc.com) controls the modulation of sunlight and laser operation, and a Raspberry Pi 3 Model B (raspberrypi.org) controls the touch-screen user interface (Adafruit, HDMI 7″ display backpack with touchscreen).

The components connect to plates that slide into rails that have been installed into protective cases (Seahorse, S630) as shown in Fig. 4. These cases (dimensions: 44.55 cm × 36.17 cm × 19.05 cm) were selected because

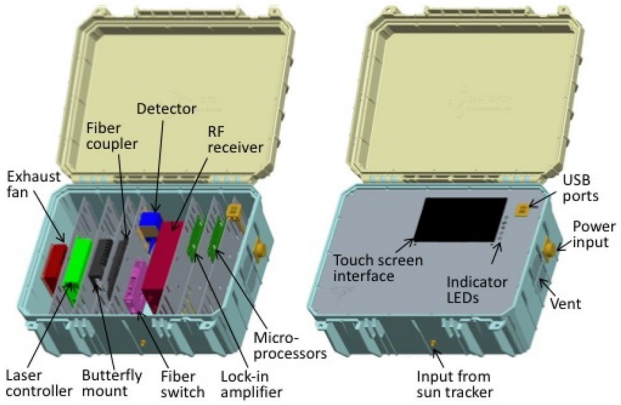

Fig. 4 The portable mini-LHR is built into a ruggedized 44.55 cm × 36.17 cm × 19.05 cm case that is cooled with a low-power exhaust fan located near the laser. For easy access, components are mounted on plates that slide into vertical rails in the case. The instrument interface is a touch screen and data can be collected through either the USB port or over WiFi

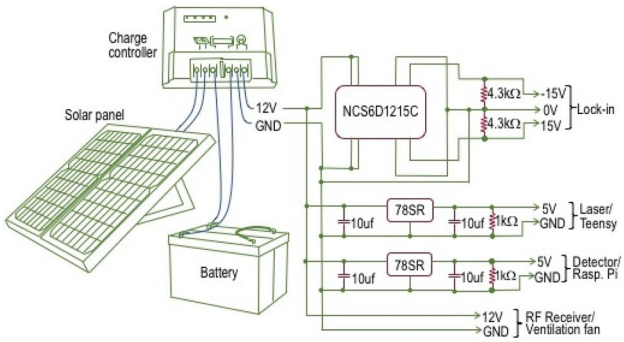

Fig. 5 The mini-LHR is powered by a simple, low-cost solar panel system that includes a 12 V battery and a charge controller that shuts the system down if the battery charge gets too low. The charge distribution board converts the 12 V to the ± 15 V needed for the lock-in amplifier as well as 5 V need for most of the other components. DC/DC converter part numbers are shown in red boxes (Murata Power Solutions)

they strap into an accessory backpack/harness system so that they can be carried into the field across rugged terrain. To power the mini-LHR in these off-grid locations, we designed a simple power module (shown in Fig. 5) that includes a 30 W folding solar panel (Ironton, #49686), a 450 W/30 A digital charge controller (Strongway, #49685), a 12 V, 12 A hour rechargeable sealed lead acid battery (Power Sonic, PS-12100) and a charge distribution board to produce the voltages needed for the various components in the instrument. The battery, charge controller, and charge distribution board are all housed in a low-cost marine battery box to keep components dry.

Users operate the mini-LHR through the touch screen interface (shown in Fig. 4) to initiate scanning of the laser and the collection of data. The mini-LHR can be operated in various automated modes for short or long duration data collection, and the user can select the wavelength range (within the capability of the laser) and resolution of the scans. Data can be accessed either via WiFi or a surface-mount USB port. If WiFi is not available and data cannot be regularly collected via USB, the mini-LHR can hold about a month's worth of data files collected in long-duration mode.

The mini-LHR can be operated routinely between 0 and 40 °C (32–104 °F). For rooftop applications where the temperature can easily exceed 40 °C, we have expanded this range by housing the mini-LHR case in a thermoelectrically cooled insulated box. For cold-weather applications < 0 °C, we have a similar insulated set-up. With ~ R19 insulation, the electronics provide enough heat to keep the mini-LHR operational down to about − 10 °C.

Which gases that the mini-LHR monitors can be varied through choice of the distributive feedback (DFB) laser; the target wavelengths of which can be custom ordered from the manufacturer. If gases have absorption features that can be measured between 1550 and 1650 nm, no major changes need to be made to the optical or electronic mini-LHR design. Gases that fall at longer wavelengths may require more significant modifications. We scan our current laser from 1.6402 to 1.6405 µm in 0.0000015 µm increments. This region is optimized for CH_4 which has a strong absorption feature at ~ 1.640375, 1.640415 µm but also captures a smaller adjacent CO_2 line at ~ 1.640415 µm.

3 Analysis of data

Production of half or full-hour data products that report CH_4 and CO_2 column mole fractions is a multi-step process that involves (1) removal of outliers in raw scans, (2) averaging raw scans into half or 1-h data blocks, (3) converting averaged scans into transmittance vs. wavelength scans, (4) mathematically simulating what the mini-LHR observes in the atmosphere, (5) fitting the simulation to the data by perturbing CH_4 and CO_2 abundancies.

The majority of outliers are caused by periodic adjustments in the sun tracker and large clouds passing overhead. In "BCLSUN" mode, the computer in the AERONET sun tracker points at the sun by calculating its location and then by fine-tuning the pointing through a quad tracker that adjusts the pointing every 30 s. This adjustment adds a repeating spike in the raw data scans. Similarly, large clouds in an otherwise clear sky will produce a sudden transmission drop. In addition, sometimes raw scans are taken when the tracker is not pointing at the sun (for example when the tracker has moved into a calibration mode related to AOD measurements and is pointing at a different portion of the sky) and these scans are discarded. After removing outliers,

scans are averaged. Half-hour averages include scans from 15 min before and 15 min after the time stamp of the data file. Similarly, full-hour averages include scans from 30 min before and 30 min after the time stamp.

The *y*-axes of the scans are the output voltage from the lock-in amplifier which is a measure of the signal intensity (I). Because laser power increases linearly with wavelength, a linear regression is fit through the baseline regions of the scan (that are not impacted by absorption or solar irradiance). This linear fit, denoted Io, is used to convert the *y*-axis to transmittance (I/I_o) [17]. The *x*-axis of the scans are related to wavelength through a prior laser characterization that relates input voltages to the laser controller to wavelength.

Spectra that the mini-LHR observes in the atmosphere is simulated using the planetary spectrum generator (PSG) which is an online tool developed at NASA GSFC [18, 19]. PSG can be used for synthesizing Earth and planetary spectra (atmospheres and surfaces) over a broad range of wavelengths (0.1 μm to 100 mm) for any observatory, orbiter or lander. Spectra are simulated by combining several state-of-the-art radiative transfer models, spectroscopic databases and planetary databases. The PSG code includes refraction of sunlight through the atmosphere as well as a computationally efficient scattering package that incorporates the latest radiative transfer numerical methods [19, 20], and is parameterized for LTE (local-thermodynamic equilibrium) calculations. The PSG is operated remotely by employing a versatile online application program interface (API). The API operates by sending a configuration file to the PSG servers. Upon reception of the configuration file, PSG computes and returns the spectra.

Part of this simulation includes the inclusion of the modern-era retrospective analysis for research and applications, version 2 (MERRA-2) data set which provides meteorological inputs [21, 22] such as modeled surface pressure for calculating dry-air columns. Our code computes temperature (T) and pressure (P) abundances for Earth by first selecting a set of six standard profiles based on season and latitude: 'Tropical', 'Midlatitude-Summer', 'Midlatitude-Winter', 'Subarctic-Summer', 'Subarctic-Winter', 'US-Standard'. These profiles provide abundances for a myriad of species and basic temperature and pressure profiles. The code then extracts P, T, O_3, H_2O and water ice abundances from the MERRA database for this location and time. Because the MERRA-2 grid is relatively rough, it does not contain fine elevation information and therefore the GTOPO30 topography database (~ 1 km resolution) is also used to refine the elevation model at the mini-LHR site. The information from MERRA-2 lat/lon is then refined in elevation (using scale-heights, etc.) using this high-resolution map.

Our code generates an initial configuration file that establishes the location and date/time of the measurement. Using this configuration file, the code calls the PSG/API and this returns all of the geometry parameters (air mass, phase angle, etc.) and an a priori vertical profile based on the date and location. Then, using this configuration file, the program goes into the fitting routine that calls the PSG/API to get calculate spectra by fitting the CO_2 and CH_4 abundances. The fit perturbs each of these abundances and obtains a fit based on the Levenberg–Marquardt algorithm which is an iterative least-squares curve fitting procedure [23, 24].

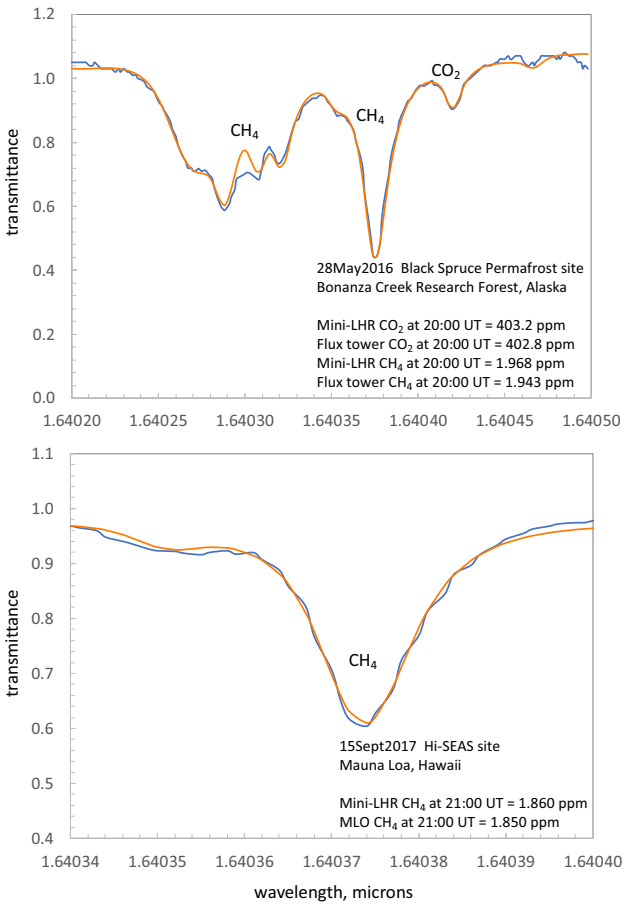

Fig. 6 Two sample mini-LHR half-hour column data products. Data are shown in blue and the PSG retrieval fit is shown in orange. The top panel (from the Bonanza Creek site) shows a scan over a broader wavelength range that includes both CH_4 and CO_2 absorption features. The bottom panel shows a narrow wavelength scan from the Hi-SEAS site that captures CH_4. The scan length and resolution is selectable from the touch screen. Both observations show good agreement with nearby surface measurements

Sample half-hour mini-LHR data products are shown in Fig. 6 from the Black Spruce site at Bonanza Creek and from the Hi-SEAS site on Mauna Loa. Data is shown in blue with the PSG algorithm fit in orange. At the Black Spruce site, cavity ring-down gas analyzer (Picarro) is co-located at the site (visible in Fig. 1). The closest surface measurement to the Hi-SEAS site is further up the mountain at Mauna

Loa Observatory which is about 0.9 km higher in altitude [25–28]. While both show good agreement between the column and surface observations, they may be misleading because the column is subject to transport and chemistry and should be viewed as rough comparisons.

4 Performance

For its size and cost (suitcase-sized and under $10 K to produce), the mini-LHR has reasonably high precisions of better than 20 ppb for CH_4 and 1 ppm for CO_2 (estimate based on the standard deviation between the data and model). The spectral resolution is selectable by the user and is typically in the range of 3×10^{-6} µm for a resolving power ($\lambda/\Delta\lambda$) greater than 500,000 at 1.64 µm. While we have not yet completed a long-term comparison with TCCON [7, 29] (planned as soon as funding is available), we have completed two short-duration comparisons of a few days each with earlier versions of the mini-LHR that measured CO_2. Because the mini-LHR was still being developed, we planned these trips as quick operational checks and to see if the amplitude of the absorption features did indeed track the changing XCO_2 that was being observed by TCCON (which they did). Functionally, this early mini-LHR was similar to the current version in that it used the same optical design, laser type and detector. However, the laser controller, lock-in amplifier, and software for operating the instrument were commercial products intended for benchtop use and they were not optimized for our application [2, 4, 6].

The first comparison (Fig. 7, top panel) took place in mid-September 2012 at the Park Falls, WI TCCON site. In this version of the mini-LHR, scans were slow (~ 10–15 min each) due mainly to the non-optimized commercial software. Consequently, we only ended up with a few scans to average which produced a somewhat noisy 1-h average. By the time of the Caltech TCCON comparison in 2014, we had made significant improvements that brought the scan time down to ~ 2 ½ min. Figure 7 (bottom panel) shows a half-hour average with less noise than the 1-h scan from 2012.

At the time that we took these data sets, the PSG retrieval tool did not exist and we were not able to analyze the data for a XCO_2 value. We have since started the process of analyzing the older data sets such as these TCCON comparisons. In Fig. 7, data is shown in blue and the PSG fit is shown in orange. As you might expect, the agreement with TCCON retrieval is better in the later data set where we could scan faster and average more scans over a shorter span of time. While the data is in good agreement, it is important to note that TCCON uses different a priori and meteorological profiles and could impact the agreement as well as differences inherent to the different types of instrument (resolution, field-of view, etc.). The CO_2 averaging kernel was recently

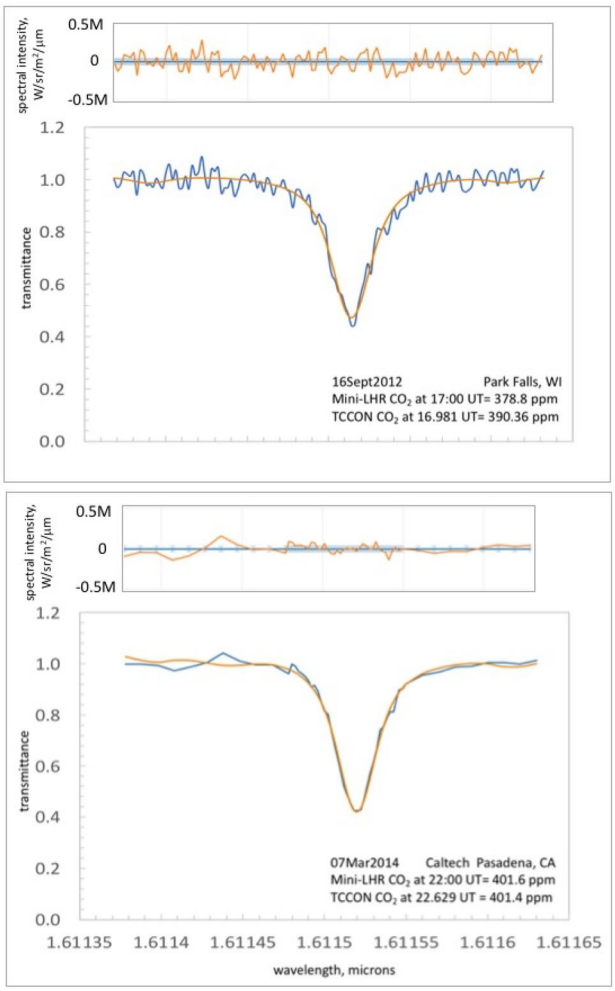

Fig. 7 Sample analyzed data from two short-duration side-by-side comparisons of earlier versions of the mini-LHR and TCCON instruments. Mini-LHR data is shown in blue with the PSG retrieval fit in orange. Above each data set shows the noise input to the model in blue and residuals in orange—verifying the absence of structure. The 2012 data are the average of three scans collected over the period of an hour and the 2014 data are the average of five scans collected over the period of a half hour. The resulting XCO2 value for the mini-LHR and the nearest corresponding value for TCCON (version GGG2014) are shown inset

calculated for the mini-LHR [30] for different solar zenith angles (SZA) assuming a SNR of 500 and found these to be similar to TCCON XCO2 retrievals of version GGG2014.

5 Insensitivity to clouds and aerosols

For passive satellite observations, scattering from clouds and aerosols is known to be significant error sources in the retrieval of column CO_2 and CH_4 [31–33]. There is, however, a misconception that ground-based passive measurements

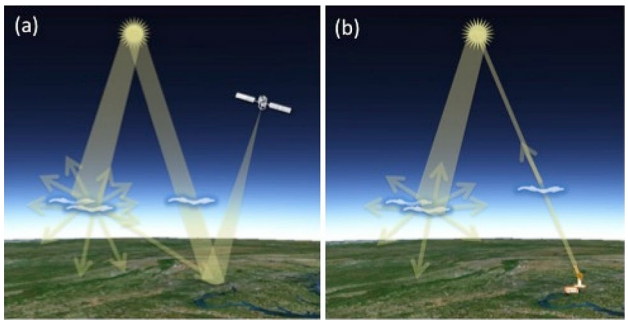

Fig. 8 In nadir-pointing satellite observations (**a**), error is introduced when scattering from clouds and aerosols changes the pathlength of sunlight through the atmosphere. In sun-tracking instruments such as the mini-LHR and TCCON (**b**), the narrow field-of-view prevents scattered light from entering the instrument. However, scattering due to extinction does reduce signal levels which impacts the signal-to-noise ratio

such as the TCCON FTS and the mini-LHR are also subject to these same errors.

Aerosols (dust/ice/clouds/hazes) cause light to scatter in a complex pattern depending on the viewing angle, aerosol size/shape and composition. The main reason that atmospheric scattering impacts passive, nadir-pointing satellite observations is that when the sun is scattered by clouds or aerosols, the path length that the sun travels to the observation spot on the ground has changed, as shown by Fig. 8a. Because the path length of sunlight through the atmosphere directly impacts the absorbance of CO_2 and CH_4 (and other atmospheric gases), this complicates the retrieval. In contrast, ground-passive measurements have a narrow field-of-view and point directly at the sun as shown by Fig. 8b. The TCCON at Park Falls, WI for example, has a field-of-view of ~ 0.14° and mini-LHRs have a field-of-view (FOV) of ~ 0.2° (compared to the sun which has a field of view of ~ 0.5°). Because the FOVs of these instruments are narrower than that of the sun, their light collection optics do not accept the scattered light outside of this FOV. Consequently, the mini-LHR and TCCON are mainly impacted by extinction which lowers the flux reaching the instrument but does not impact the relative absorption of the atmospheric gases.

Inclusion and realistic treatment of scattering phenomenon in the radiative transfer analysis is extremely computationally expensive, yet several approaches to attack this problem do exist. The efficient scattering package available in PSG incorporates the latest radiative transfer numerical methods, and it is parameterized for LTE (local-thermodynamic-equilibrium) calculations using HITRAN spectroscopic [19, 20]. We use the PSG to simulate the difference in the effect scattering on nadir satellite retrievals and ground-based sun-viewing measurements.

We compare scattering due to clouds, dust, and water–ice over a narrow wavelength (1.640–1.641 μm) for the upward

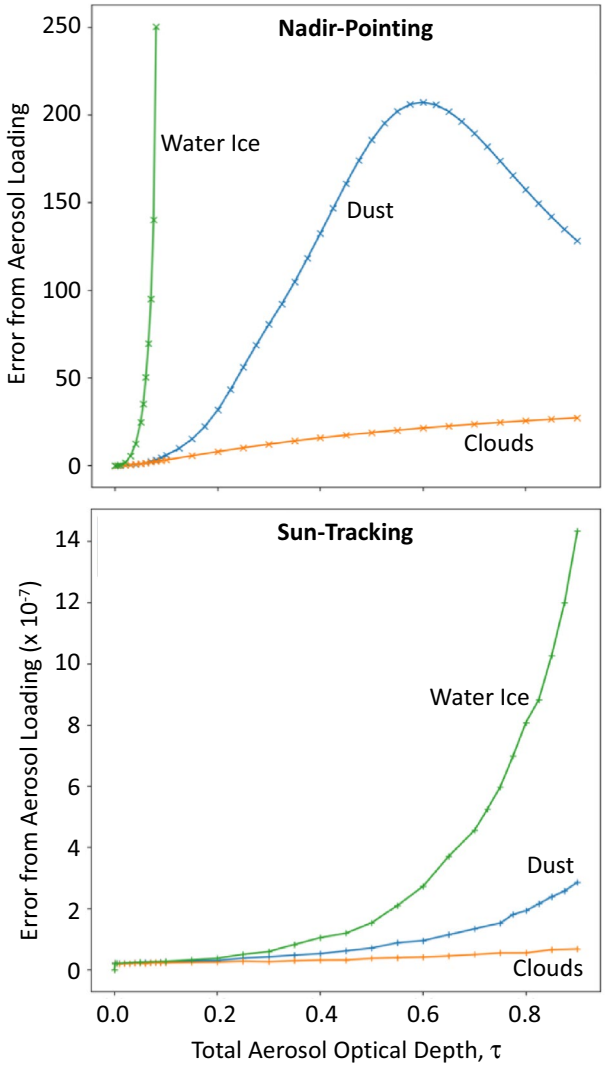

Fig. 9 Error from aerosol loading. The impact of dust, cloud, and water ice aerosols on column retrievals is simulated for different observing geometries over typical ranges of aerosol optical depth (AOD). The error from aerosol loading is the standard deviation between spectra generated with and without aerosols present. The impact of aerosols on upward-viewing, sun-pointing instruments is not significant, while the impact of aerosols on nadir viewing instruments is apparent at levels as low as $\tau = 0.02$

pointing mini-LHR with a 0.2° field-of-view, and a nadir-pointing satellite similar to OCO-2 with a 705 km orbit, a 1 mile diameter spot size on the ground, two stream-pairs, and two azimuths. In Fig. 9, using the PSG code, we have simulated the error as the standard deviation between a spectra generated with and without aerosol loading as a function of total optical depth of the aero sol added (τ). Average aerosol optical depth (AOD) in the US typically ranges from 0.1 to 0.15, however, AOD is typically higher than this in regions where there is limited data such as the tropics or in heavily polluted cities where AOD can exceed 1.0. Standard

deviations for upward-viewing instruments such as the mini-LHR and TCCON are negligible over the entire range of optical depths because scattered light is outside of the field-of-view of the light collection optics, while standard deviations for the nadir-viewing instrument that observes an illuminated spot on the ground become significant at optical depths as low as 0.02. The impact of clouds and aerosols on the upward-viewing geometry is primarily extinction, resulting in lower levels of sunlight reaching these ground instruments. While this does not add error to the collected spectra, it does impact the signal level and consequently signal-to-noise levels.

6 Future improvements

In addition to a long-term TCCON comparison discussed earlier, we will be adding a calibration step to the mini-LHR data analysis to track performance and establish documented traceability of column data products. Calibrations and validations will establish and report measurement precision, measurement bias, and measurement error as defined by the Bureau International des Poids et Measures (BIPM)/Joint Committee for Guides in Metrology (JCGM) [34]. The calibration procedure will involve the mini-LHR instrument scanning a NIST (National Institute of Standards and Technology) traceable atmospheric mixture of gases in an absorption cell using a second DFB laser as the incoming light (instead of sunlight). Measurement precision will be found by tracking the standard deviation of repeated scans. In addition, any measurement bias or systematic error will be tracked by these regular repeated calibrations.

An estimate of measurement error will be found through a future side-by-side comparison of column data products from the Mini-LHR and the TCCON FTS located at NASA Armstrong Flight Research Center (AFRC) at Moffett Field, CA. The TCCON FTS measures column CH_4 and CO_2 at the same wavelengths but lower resolution as the mini-LHR. While TCCON has a well-documented history of characterization, we refer to this as an "estimate" of measurement error due to differences in resolution and because there are known biases between TCCON sites (1% for CO_2 and 2% for CH_4 in US sites and $1.1\% \pm 0.2\%$ for CO_2 at European sites) [29, 35].

7 Conclusions

We have presented an updated design for our portable mini-LHR design as well as sample column measurements of CO_2 and CH_4 observed at two geographically distinct field sites in Alaska and Hawaii. Data were analyzed using the Planetary Spectrum Generator (PSG) retrieval to produce column mole fractions; both sites showed good agreement with co-located surface observations. This newly available PSG retrieval product also made it possible to analyze two data sets using earlier versions of the mini-LHR during side-by-side comparisons with TCCON; these also showed reasonable agreement.

The updated version of the mini-LHR has a resolving power ($\lambda/\Delta\lambda$) greater than 500,000 at 1.64 μm with precisions of better than 20 ppb and 1 ppm for CH_4 and CO_2, respectively. Because it operates autonomously and does not require electricity, the mini-LHR can be easily deployed to geographically challenging locations that do not have infrastructure and where other column observations are not possible and where there are gaps in the carbon record such as the Amazon river basin and Africa. In addition, because mini-LHR instruments are portable and can be co-located, they can be used to characterize bias between larger, stationary, column observing instruments. Mini-LHR instruments can also be deployed quickly to respond to transient events such as methane leaks or can be used for field studies targeting geographical regions.

Acknowledgements We would like to thank Jared Entin and the NASA Interdisciplinary (IDS) Program (Grant number 12-IDS12-0024, NRA: NNH12ZDA001N-IDS. Since gov, DUNS # is 004968611-CAGE: 36FC1), Eugenie Euskirchen and Colin Edgar at the University of Alaska Fairbanks, the Hi-SEAS V Crew, Jake Bleacher, Brent Holben and the AERONET team, Paul Wennberg, Coleen Roehl, and Deborah Wunch from TCCON, and former team members Greg Clarke and Hilary Melroy for help collecting data at TCCON sites.

References

1. E. L. Wilson, M. L. McLinden, Miniaturized laser heterodyne radiometer for carbon dioxide, methane and carbon monoxide measurements in the atmospheric column, (Filed 2012). U.S. Patent No. 8699029, awarded on 15 Apr 2014
2. H.R. Melroy, E.L. Wilson, G.B. Clarke, L.E. Ott, J.-P. Mao, A.K. Ramanathan, M.L. McLinden, Autonomous field measurements of CO_2 in the atmospheric column with the miniaturized laser heterodyne radiometer (mini-LHR). Appl. Phys. B **120**, 609–615 (2015)
3. G. B. Clarke, E. L. Wilson, P. Palmer, L. Feng, J. P. Mao, A. Ramanathan, L. Ott, B. N. Duncan, H. R. Melroy, S. R. Kawa, M. L. McLinden, B. N. Holben, and A. J. DiGregorio, The science and technology case for a global network of compact, low cost ground-based laser heterodyne radiometers for column measurements of CO_2 and CH_4. American Geophysical Union (AGU) Fall Meeting (2015)
4. E.L. Wilson, M.L. McLinden, J.H. Miller, G.R. Allen, L.E. Ott, H.R. Melroy, G.B. Clarke, Miniaturized laser heterodyne radiometer for measurements of CO_2 in the atmospheric column. Lasers Opt. Appl. Phys. B **114**, 385–393 (2013). https://doi.org/10.1007/s00340-013-5531-1

5. E.L. Wilson, A.J. DiGregorio, V.J. Riot, M.S. Ammons, W.W. Bruner, D. Carter, J.-P. Mao, A. Ramanathan, S.E. Strahan, L.D. Oman, C. Hoffman, R.M. Garner, A 4 U laser heterodyne radiometer for methane (CH_4) and carbon dioxide (CO_2) measurements from an occultation-viewing CubeSat. Meas. Sci. Technol. **28**, 035902 (2017)
6. G.B. Clarke, E.L. Wilson, J.H. Miller, H.R. Melroy, Uncertainty analysis for the miniaturized laser heterodyne radiometer (mini-LHR). Meas. Sci. Technol. **25**, 055204–055209 (2014)
7. D. Wunch, G.C. Toon, F. Blavier, L.R.A. Washenfelder, J. Notholt, B. Connor, D.W.T. Griffith, V. Sherlock, P.O. Wennberg, The total carbon column observing network (TCCON). Philos. Trans. R. Soc. Math. Phys. Eng. Sci. **369**, 2087–2112 (2011)
8. R. T. Menzies, M. S. Shumate, Usefulness of the infrared heterodyne radiometer in remote sensing of atmospheric pollutants. Joint Conference on sensing of environmental pollutants, pp. 1–4 (1971)
9. D. Weidmann, W.J. Reburn, K.M. Smith, Retrieval of atmospheric ozone profiles from an infrared quantum cascade laser heterodyne radiometer: results and analysis. Appl. Opt. **46**, 7162–7171 (2007)
10. A. Delahaigue, D. Courtois, C. Thiebeaux, S. Kalite, B. Parvitte, Atmospheric laser heterodyne detection. Infrared Phys. Technol. **37**, 7–12 (1996)
11. R.K. Seals Jr., Analysis of tunable laser heterodyne radiometry: remote sensing of atmospheric gases. AIAA J. **12**, 1118–1122 (1974)
12. V. Zeninari, B. Parvitte, D. Courtois, A. Delahaigue, C. Thiebeaux, An instrument for atmospheric detection of NH3 by laser heterodyne radiometry. J. Quant. Spectros. Radiat. Transfer **59**, 353–359 (1998)
13. R.T. Menzies, A re-evaluation of laser heterodyne radiometer ClO measurements. Geophys. Res. Lett. **10**, 729–732 (1983)
14. R. T. Menzies, Monitoring atmospheric pollutants with a heterodyne radiometer transmitter-receiver, United States Patent, Patent number 3,766,380 (1973)
15. B.N. Holben, D. Tanre, T.F. Eck, I. Slutsker, N. Abuhassan, W.W. Newcomb, J. Schaefer, B. Chatenet, F. Lavenue, Y.J. Kaufman, J. Vande Castle, A. Setzer, B. Markham, D. Clark, R. Frouin, R. Halthore, A. Kamieli, N.T. O'Neill, C. Pietras, R.T. Pinker, K. Voss, G. Zibordi, An emerging ground-based aerosol climatology: aerosol optical depth from AERONET. J. Geophys. Res. **106**, 67–97 (2001)
16. B.N. Holben, T.F. Eck, I. Slutsker, D. Tanre, J.P. Buis, A. Setzer, E. Vermote, J.A. Reagan, Y.J. Kaufman, T. Nakajima, F. Lavenue, I. Jankowiak, A. Smirnov, AERONET—a federated instrument network and data archive for aerosol characterization. Remote Sens. Environ. **66**, 1–16 (1998)
17. E. L. Wilson, Field results from 3 campaigns to validate the performance of the miniaturized laser heterodyne radiometer (mini-LHR) for measuring carbon dioxide and methane in the atmospheric column, Fall Meeting of the American Geophysical Union Proceedings, San Francisco, CA (2013)
18. G. L. Villanueva, M. Smith, M. J. Wolff, S. Protopapa, T. Hewagama, A. M. Mandell, S. Faggi, Planetary spectrum generator (PSG). https://psg.gsfc.nasa.gov (2019)
19. G.L. Villanueva, M.J. Mumma, R.E. Novak, H.U. Kaufl, P. Hartogh, T. Encrenaz, A. Tokunaga, A. Khayat, M.D. Smith, Strong water isotopic anomalies in the martian atmosphere: probing current and ancient reservoirs. Science **348**, 218–221 (2015)
20. M. D. Smith, M. J. Wolff, R. T. Clancy, and S. L. Murchie, Compact reconnaissance imaging spectrometer observations of water vapor and carbon monoxide, J. Geophys. Res. 114 (2009). https://doi.org/10.1029/2008JE003288
21. R.H. Reichle, R.D. Koster, G.J.M. DeLannoy, B.A. Forman, Q. Liu, S.P.P. Mahanama, A. Toure, Assessment and enhancement of MERRA land surface hydrology estimates. J. Clim. **24**, 6322–6338 (2011)
22. M.M. Rienecker et al., MERRA: NASA's modern-era retrospective analysis for research and applications. J. Clim. **24**, 3624–3648 (2011)
23. K. Levenberg, A method for the solution of certain non-linear problems in least squares. Am. Math. Soc. **2**, 164–168 (1944)
24. D.W. Marquardt, An algorithm for least-squares estimation of nonlinear parameters. J. Soc. Ind. Appl. Math. **11**, 431–441 (1963)
25. W.D. Komhyr, T.B. Harris, L.S. Waterman, Atmospheric carbon dioxide at mauna loa observatory NOAA global monitoring for climatic change measurements with a nondispersive infrared analyzer, 1974–1985. J. Geophys. Res. **94**, 8533–8547 (1989)
26. K.W. Thoning, P.P. Tans, Atmospheric carbon dioxide at mauna loa observatory: analysis of the NOAA GMCC data 1974–1985. J. Geophys. Res. **94**, 8549–8565 (1989)
27. E.J. Dlugokencky, L.P. Steele, P.M. Lang, K.A. Masarie, Atmospheric methane at Mauna Loa and Barrow observatories: presentation and analysis of in-situ measurements. J. Geophys. Res. **100**(23), 103–123 (1995)
28. K. A. Masarie, L. P. Steele, P. M. Lang, A rule-based expert system for evaluating the quality of long-term, in situ, gas chromatographic measurements of atmospheric methane, NOAA Tech. Memo. ERL CMDL-3, NOAA Environ Res. Lab, Boulder, Colorado (1991)
29. D. Wunch, G.C. Toon, P.O. Wennberg, S.C. Wofsy, M. Stephen, M.L. Fischer, O. Uchino, J.B. Abshire, P.F. Bernath, S.C. Biraud, F. Blavier, L.C. Boone, K.P. Bowman, E.V. Browell, T. Campos, B.J. Connor, B.C. Daube, N.M. Deutscher, M. Diao, J.W. Elkins, C. Gerbig, E. Gottlieb, D. Griffith, D.F. Hurst, R. Jimenez, G. Keppel-Aleks, E.A.I. Kort, S. Park, J. Robinson, C.M. Roehl, Y. Sawa, V. Sherlock, C. Sweeney, T. Tanaka, M.A. Zondo, Calibration of the total carbon column observing network using aircraft profile data. Atmos. Meas. Tech. **3**, 1351–1362 (2010)
30. P.I. Palmer, E.L. Wilson, G.L. Villanueva, G. Liuzzi, L. Feng, A.J. DiGregorio, J.-P. Mao, L. Ott, B.N. Duncan, Potential improvements in global carbon flux estimates from a network of laser heterodyne radiometer measurements of column carbon dioxide. Atmos. Meas. Tech. **12**, 2579–2594 (2019)
31. O. Uchino, N. Kikuchi, T. Sakai, I. Morino, Y. Yoshida, T. Nagai, A. Shimizu, T. Shibata, A. Yamazaki, A. Uchiyama, N. Kikuchi, S. Oshchepkov, A. Bril, T. Yokota, Influence of aerosols and thin cirrus clouds on the GOSAT-observed CO_2: a case study over Tsukuba. Atmos. Chem. Phys. **12**, 3393–3404 (2012)
32. I. Aben, O. Hasekamp, W. Hartmann, Uncertainties in the space-based measurements Of CO2 columns due to scattering in the Earth's atmosphere. J. Quant. Spectros. Radiat. Transfer **104**, 450–459 (2007)
33. J.-P. Mao, S.R. Kawa, Sensitivity studies for space-based measurement of atmospheric total column carbon dioxide using reflected sunlight. Appl. Opt. **43**, 914–927 (2004)
34. Bureau International des poids et Meaures, JCM 200:1012: International vocabulary of metrology—basic and general concepts and associated terms (VIM), 3rd edition. http://www.bipm.org/en/publications/guides/vim.html (2012). Accessed 19 Jan 2016
35. J. Messerschmidt, M.C. Geibel, T. Blumenstock, H. Chen, N.M. Deutscher, A. Engel, D.G. Feist, C. Gerbig, M. Gisi, F. Hase, K. Katrynski, O. Kolle, J.V. Lavric, J. Notholt, M. Palm, M. Ramonet, M. Rettinger, M. Schmidt, R. Sussmann, G.C. Toon, F. Truong, T. Warneke, P.O. Wennberg, D. Wunch, I. Xueref-Remy, Calibration of TCCON column-averaged CO2: the first aircraft campaign over European TCCON sites. Atmos. Chem. Phys. **11**, 10765–10777 (2011)